Carbohydrate Polymers 75 (2009) 172–179

Contents lists available at ScienceDirect

Carbohydrate Polymers

journal homepage: www.elsevier.com/locate/carbpol

Nano clay reinforced PCL/starch blends obtained by high energy ball milling

Luigi Vertuccio, Giuliana Gorrasi, Andrea Sorrentino *, Vittoria Vittoria

Chemical and Food Engineering Department, University of Salerno, via Ponte Don Melillo, I84084 Fisciano (Salerno), Italy

ARTICLE INFO

Article history:
Received 27 March 2008
Received in revised form 2 July 2008
Accepted 11 July 2008
Available online 22 July 2008

Keywords:
Nano composites
PCL/starch blends
Thermo-mechanical properties
Transport properties
Ball milling

ABSTRACT

Sodium montmorillonite was incorporated into a poly(ε-caprolactone)–starch blend by means of a ball mill. The structural organization and physical (mechanical, thermal and barrier) properties were analyzed and correlated with the milling conditions. Scanning electron microscopy and X-ray characterization show that the milling process can improve the compatibilization between the PCL and the starch phases, while promotes the dispersion of clay minerals at nanometric level. The milling time strongly influences the mechanical and barrier properties. In particular, the best results in terms of elastic modulus and permeability coefficient were achieved with a complete delamination of the pristine clay structure. In summary, the milling process not only has demonstrated to be a promising compatibilization method for immiscible PCL–starch blends, but it can be also used to improve the dispersion of nanoparticles into the polymer blends.

1. Introduction

Demand for degradable and biocompatible polymers is rapidly increasing, especially in the packaging sector where it is highly encouraged by environmental management policies (Flemming, 1998; Orhan & Büyükgüngör, 2000). Poly(ε-caprolactone) (PCL) is synthetic, biodegradable polyester that is compatible with many types of polymers and it is one of the most promising biodegradable polymers currently available on the market (Hung & Edelman, 1995; Li & Vert, 1995). High cost and low melting temperature ($T_m \approx 60\,°C$) are, however, the main limitations preventing the PCL widespread industrial use. To overcome these problems, PCL is usually mixed with other low cost biodegradable polymers (De Kesel, Vander Wauven, & David, 1997; Nakayama et al., 1997; Oya, Kurokawa, & Yasuda, 2000).

Starch is a non-expensive, renewable polymer that is a potential raw material for the manufacturing of plastic-like materials. However, starch based plastics have poor long-term stability caused by water absorption, poor mechanical properties and difficult processability.

It was demonstrated that the addition of small quantities of inorganic material dispersed at nanometric level is one of the most promising strategies to improve physical and mechanical properties of polymers and blends (Giannelis, 1996). The obtained nano-hybrid composites possess unusual properties, very different from their microscale counterparts. They often show improved mechanical and oxidation stability, barrier properties, decreased solvent uptake, self-extinguishing behavior and, eventually, tuneable biodegradability (Alexandre & Dubois, 2000). The nanometric dispersion, generally, is achieved following one of these two approaches: (1) dispersion of nanoparticles in suitable monomers and subsequent polymerization or (2) direct incorporation of nanoparticles in the polymer chains from either solution or melt (Alexandre & Dubois, 2000; Giannelis, 1996). For most natural or biodegradable polymers these approaches are not always allowed. In fact, the melting temperature of these polymers is too close to the temperature at which thermal degradation takes place, whereas the use of solvents are strongly limited by the problems correlated with the gelation process.

Several studies have demonstrated that solid-state milling of polymeric materials represent a strategy for producing polymer blends with acceptable mechanical properties. Mechanical milling applied to polyamide, polystyrene and polyethylene have shown that this treatment resulted in considerable alteration of both crystal structure and microstructure (Pan & Shaw, 1994). When applied to polymeric mixtures it has proven to improve the compatibilization between the different components and increase the degree of dispersion and (Nesarikar, Khait, & Mirabella, 1997; Smith et al., 2000). The combination of mechanical effects, such as impact, compressive and shear forces, is expected to induce radical chain scissions within polymer particles (Cavalieri, Padella, & Bourbonneux, 2002). Reaction of macromolecular free radicals, from different chain species of intrinsically incompatible polymer could couple and produce a more stable blend by grafting.

Very recently, it has been proved by the authors that High Energy Ball Milling (HEBM) can help to obtain novel nano-composites

---

* Corresponding author. Tel.: +39 089 96 4013; fax: +39 089 96 4057.
E-mail address: asorrentino@unisa.it (A. Sorrentino).

0144-8617/$ - see front matter © 2008 Elsevier Ltd. All rights reserved.
doi:10.1016/j.carbpol.2008.07.020

with new characteristics, difficult to obtain by other conventional techniques (Gorrasi et al., 2007; Mangiacapra, Gorrasi, Sorrentino, & Vittoria, 2006; Sorrentino et al., 2005).

In this paper we propose the HEBM as an alternative preparation method for PCL–starch–clay composites. The clay dispersion was promoted by the energy transfer between milling balls and polymer/clay mixture, which in turn results grinded and intimately mixed. The structural organization and physical (mechanical, thermal and barrier) properties were studied and correlated with the milling conditions.

2. Experimental

2.1. Materials

- Commercial grade poly(ε-caprolactone) (CAPA® 6501) was supplied by Solvay in form of powder (particle size less than 100 μm). The number average molar mass was 49,000 with a polydispersity of 1.4, as determined by size exclusion chromatography (Lepoittevin et al., 2002).
- High amylase maize starch (AmyloGel® 03003) was kindly supplied by Cargill, Italy. The amylose content was ranging between 60 and 80%, whereas the protein content was less than 0.7%.
- The clay mineral (Na^+-Montmorillonite) was supplied by "Sud-Chemie AG", Moosburg, Germany.

2.2. Samples preparation

2.2.1. Incorporation of Clay into PCL–starch: HEBM procedure

Samples in powders form were milled at ambient temperature in a *Retsch* Centrifugal Ball Mill (model S 100). The steel milling jar of 50 cm^3 was loaded with 4 g of polymer and 10 g of steel balls (5 balls of 10 mm of diameter). Milling was conducted for three different times (4, 7, 10 h) at the rotation speed of 580 rpm. As reported in Table 1, various blends formulations with different PCL–starch–clay ratios were obtained and analyzed.

2.3. Films preparation

The samples obtained by milling process were moulded in a Carver laboratory press, at the temperature of 120 °C, followed by air cooling. Films 100–110 μm thick were produced and stored in a closed chamber over hygroscopic salts for 1 week, before each characterization test.

2.4. Characterization methods

The thermal stability of the neat PCL, the Starch and the different blends was determined on powder samples. The thermo-gravimetric analysis (TGA) was carried out with a *Mettler Toledo* (TC-10) thermo-balance, under air flow. The mass of each sample was 7–9 mg. The thermo-gravimetric curves were recorded in the course of heating from 25 °C to 800 °C at a rate of 10 °C/min.

Table 1
Samples codification

Sample	Composition	Time of milling
PCL100ST0C0T4	PCL(100%wt.)	4 h
PCL60ST40C0T4	PCL(60%wt.) + Starch(40%wt.)	4 h
PCL60ST40C3T4	PCL(60%wt.) + Starch(37%wt.) + Clay(3%wt.)	4 h
PCL60ST40C3T7	PCL(60%wt.) + Starch(37%wt.) + Clay(3%wt.)	7 h
PCL60ST40C3T10	PCL(60%wt.) + Starch(37%wt.) + Clay(3%wt.)	10 h

Differential scanning calorimetry (DSC) analysis was carried out on powders samples with a mass ranging between 5 and 7 mg. The tests were carried out by means of a DTA *Mettler Toledo* (**DSC 30**) under nitrogen atmosphere. The samples were heated from 25 °C to 100 °C at 10 °C/min and kept at 100 °C for 5 min to eliminate the previous thermal history. After that, the samples were quickly cooled to the selected crystallization temperature ($T_c = 37$, 40, 43 and 45 °C) and hold at this temperature for a time long enough to allow complete crystallization.

In order to prevent a thickening effect of lamellae on the melting temperature determination, a second thermal cycle was performed. The second isothermal test at each crystallization temperature was stopped at a time such to reach about 5% of the enthalpic peak of the previous run.

The temperature was then raised up to complete fusion at 10 °C/min and the peak temperature of the melting endotherm was taken as the melting point.

X-ray diffraction (XRD) measurements were performed on the sample films by means of a *Bruker* (*D8 Advance*) X-ray diffractometer with Ni-filtered CuKα radiation ($\alpha = 1.5405$ Å).

Scanning electron microscopy (SEM) was conducted using a *JEOL* (model JSM-5900LV) scanning electron microscope. The samples films were fractured after freezing in liquid nitrogen and observed on the fractured surfaces.

Tensile tests were performed on the sample films using a dynamometric apparatus *INSTRON* (model 4301). The measurements were carried out at room temperature at a deformation rate of 2 mm/min, whereas the initial length of the samples was 10 mm. The elastic moduli were derived from the initial part of the stress–strain curves, giving to samples a deformation of 0.1%.

Thermo-mechanical properties of the different blends were determined with a dynamic thermo-mechanical analyzer *TA instrument* (DMA 2980). Film samples with dimensions 4 × 15 mm were tested by applying a variable tensile deformation. The displacement amplitude was set to 0.1%, whereas the measurements were performed at the frequency of 1 Hz. The range of temperature was from −80 °C to 40 °C at the scanning rate of 3 °C/min.

Transport properties experiments were performed using a conventional McBain spring balance system, which consists of a glass water-jacketed chamber serviced by a high vacuum line for sample degassing and penetrant removal (Felder & Huvard, 1980). Inside the chamber samples were suspended from a helical quartz spring supplied by Ruska Industries, Inc. (Houston, TX) and had a spring constant of 1.892 cm/mg. The temperature was controlled to 30 ± 0.1 °C by a constant temperature water bath. Before beginning the sorption experiments, the sample was exposed to vacuum for at least 24 h in order to remove previously sorbed air gases and water vapour from the polymer. Liquid penetrant was subjected to several freeze–thaw cycles to remove dissolved gases. Then the sample was exposed to the penetrant at fixed pressures, and the spring position was recorded as a function of time using a cathetometer. The spring position data were converted to mass uptake data using the spring constant. Diffusion coefficients were extracted from these kinetic sorption data. The data presented are averaged on three samples.

3. Results and discussion

3.1. X-Ray diffractograms

Fig. 1 shows the X-ray diffraction spectra of several film samples as well as the clay powders. The diffractogram of the sample of PCL milled 4 h shows the characteristic pattern of PCL in its crystalline structure with the well developed peaks at $2\theta = 21.3°$ and 23.7° and a shoulder peak at about 22.0° (Fig. 1b). Also the spectra of the composites, even after 10 h of milling, show that the crystal-

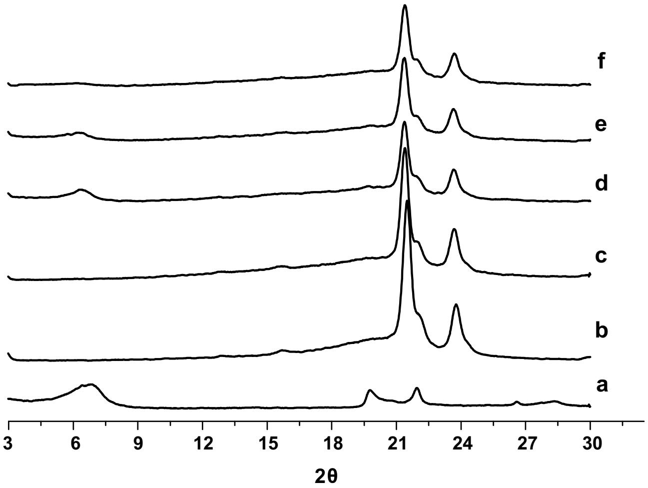

Fig. 1. X-ray powder spectra of (a) nanofil 757; (b) PCL100ST0C0T4; (c) PCL60ST40C0T4; (d) PCL60ST37C3T4; (e) PCL60ST37C3T7; (f) PCL60ST37C3T10.

line phase of PCL is well developed. It can be concluded that the chosen milling conditions are not able to affect the PCL crystalline morphology, neither when it is pure nor in blends with starch and clay.

The clay shows the main diffraction peak at $2\theta = 6.80°$, corresponding to a basal spacing of the platelets equal to 11.0 Å. From Fig. 1, it is also evident as in the composite blends this peak appears reduced in intensity going from 4 h to 7 h of milling. It completely disappears in the spectra of the composite milled for 10 h. An evident and gradual change of the clay structure occurred in the samples during the milling process, leading to a loss of the basal order (Sondi, Stubicar, & Pravdic, 1997). Probably, during milling the clay particles divide preferentially along the basal plane (i.e. in individual sheets) even if a partial rupture of the clay sheets normal to the basal plane cannot be excluded. In any case, for milling times higher than 7 h, a nanometric dispersion into the PCL–starch blends seems to occur. Even if an irrefutable proof for the effective dispersion of the clay can be obtained only with a direct inspection (TEM analysis), it should be considered that the same samples (namely the same volume) were subsequently examined by TGA (see below), thus confirming the presence of clay and its concentration.

3.2. Scanning electron microscopy

Fig. 2 shows the SEM micrographs of the pristine starch (a), the blend PCL–starch (b) and the blend with 3% clay milled for 4 (c) and 10 h (d), respectively.

In sample milled for 4 h (Fig. 2b) the starch granules maintain a spherical shape with the largest particle diameter being about 5 μm. In this case, two distinct phases are clearly observed, even if a good distribution of starch in the PCL matrix is obtained. The smooth edges of the starch particles, however, make clear the poor interaction between these particles and the PCL matrix.

Also PCL–starch–clay blend milled for 4 h (Fig. 2c) presents a fracture surface similar to that shown in Fig. 2b, indicating that clay do not produce a significant change in morphology for this milling time.

Fig. 2d illustrates the PCL–starch–clay blend milled for 10 h. In this case, it is distinctly observed that the starch granule is well embedded into the PCL matrix: the starch particles are smaller, irregular and the interface seems unclear, confirming a better interconnection between the two phases. Similar results were obtained by use of compatibilizers (Avella et al., 2000; Koenig & Huang, 1995).

3.3. Thermo-gravimetric analysis (TGA)

All samples were analyzed by thermo-gravimetric analysis, in order to determine the effective content of inorganic phase and the degradation behavior (Fig. 3).

The degradation curve of the starting starch sample present a first loss in weight at around 100 °C, due to the water loss. The first loss in weight is followed by a second main degradation step centred at about 310 °C (Fig. 3).

In contrast, the thermo-gravimetric curve of the PCL milled for 4 h shows a just one main step centred at about 430 °C. The as received PCL powders show a single degradation curve (not show in Fig. 3) identical to that of PCL milled for 4 h. It confirms that 4 h of the chosen milling conditions do not produce evident degradation in the PCL structure.

The various milled blends show an intermediate behavior, whereas the addition of 3% of clay seems to influence only the step associated with the PCL degradation. This step is, in fact, delayed of about 10 °C in all cases where the clay was present.

3.4. Thermal analysis (DSC)

The crystallization behavior of a blend, represented by its half time crystallization values, crystallinity degree and melting temperature is a very helpful tool in the miscibility investigation, change in molecular weight and nucleation effect.

The crystallinity degree (X_c) of the PCL component in the composites was determined by the melting peak area as follows (Eq. (1)):

$$X_c = \frac{\Delta H_m}{\Delta H_m^0 f} \tag{1}$$

where ΔH_m^0 is the enthalpy of fusion of the sample, ΔHf_m is the heat of fusion for 100% crystalline PCL (taken to be 139.5 J/g (Crescenzi, Manzini, Calzolari, & Borri, 1972) and f is the weight fraction of PCL.

Table 2 shows, for each sample isothermally crystallized at 37 °C, the melting temperature calculated by the maxima of the melting peaks, the heat of fusion and the crystallinity.

Sample containing 40% of starch and milled for 4 h shows the higher value of PCL crystallinity, which suggested that starch and short milling time act as nucleating agent for PCL, whereas the clay addition as well as the increase in milling time do not change significantly the final crystallinity degree of PCL. The slight decrease in the crystallinity observed in the presence of clay was probably attributable to the increased compatibility of the two polymeric systems (Koenig & Huang, 1995). Thus, these results suggested that the polymers are immiscible and that a severe milling action can help the compatibility between the two systems, whereas the nucleation effect of the starch is significantly greater than that of the clay.

From Table 2 it is also evident that there is no significant difference in the melting temperature of PCL when it was milled alone or with starch. A similar behavior was found by the equilibrium melting temperature (T_m^0), determined in according with the linear Hoffman–Weeks extrapolation.

The evolution of heat released during the course of crystallization can be used to characterize the overall kinetics of crystallization by means of the Avrami model (Eq. (2)):

$$1 - X_c(t) = \exp(-kt^n) \tag{2}$$

where, $X_c(t)$ is the relative crystallinity as a function of time (t), k is the overall crystallization rate constant, n is the Avrami exponent that depends both on the nature of the nucleation and on the growth geometry. The Eq. (2) can be linearized as follow (Eq. (3)):

$$\ln(-\ln[1 - X_c(t)]) = \ln(k) + n\ln(t) \tag{3}$$

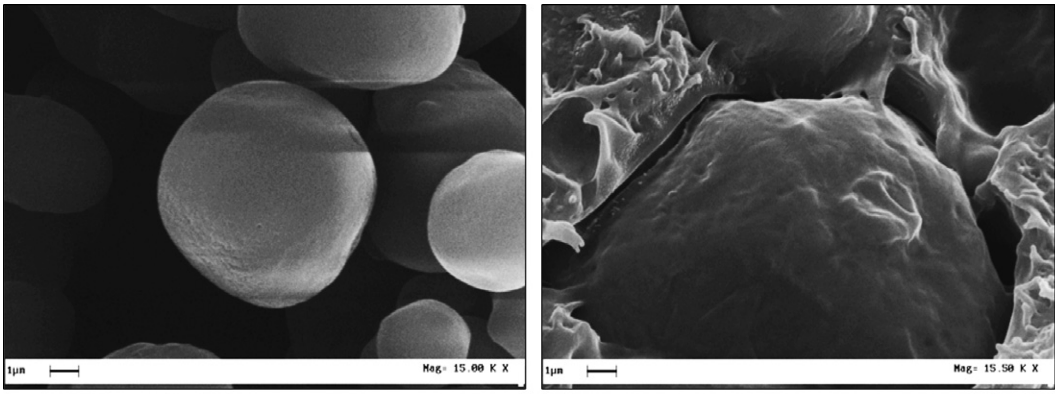

(a) Starch (b) PCL60ST40C0T4

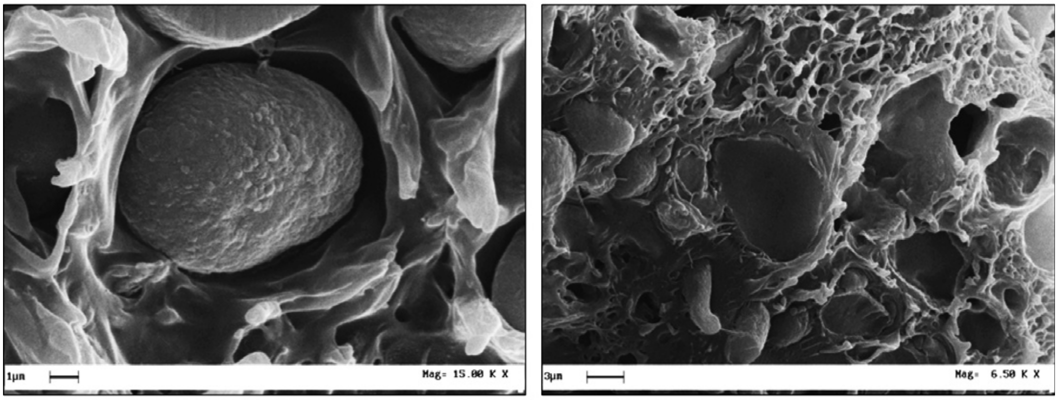

(c) PCL60ST37C3T4 (d) PCL60ST37C3T10

Fig. 2. SEM micrograph of selected samples.

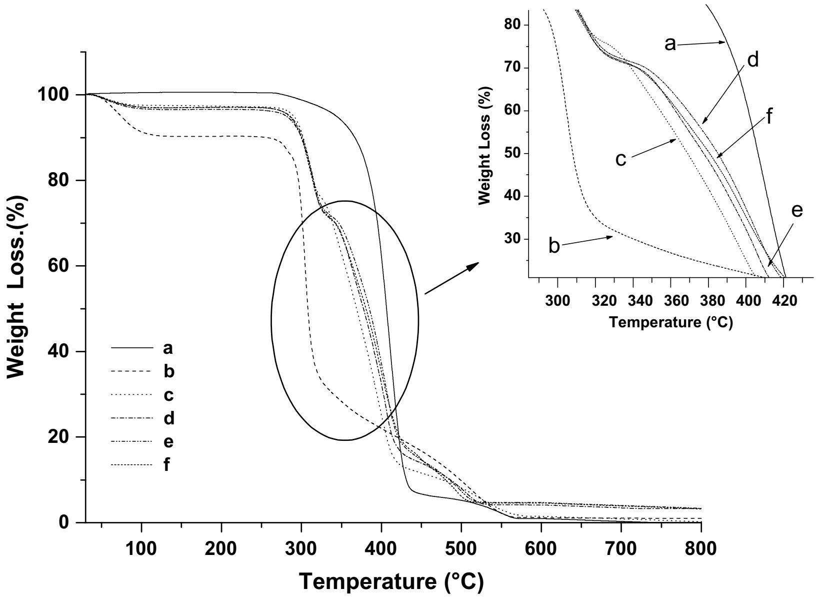

Fig. 3. Thermo-gravimetric curves of (a) PCL100ST0C0T4; (b) Starch; (c) PCL60ST40C0T4; (d) PCL60ST37C3T4; (e) PCL60ST37C3T7; (f) PCL60ST37C3T10.

From Table 3, it can be seen that for PCL and its blends, the higher the crystallization temperature, the shorter is the crystallization rate. At each crystallization temperature, the crystallisation rate of blends is much faster than that of pure PCL. This suggests again that starch in blends acts as nucleating agent, which could enhance the crystallisation rate of PCL. The milling time as well as the clay addition has similar effects on the crystallization behavior, even if they are much less effective in comparison to the starch.

The overall effect of the addition of an immiscible polymer on crystallization rate of a crystallizable macromolecule depends on the values of the energy barriers that need to be

Table 2
Thermal analysis of PCL and its blends isothermally crystallized at 37 °C

Samples	T_m [°C]	LHW T_m^0	ΔH_m [J/g]	X_c [%]
PCL	57.7	65.7	59.5	42.6
PCL100ST0C0T4	57.7	65.5	58.3	41.8
PCL60ST40C0T4	57.7	65.5	67.4	48.3
PCL60ST37C3T4	57.9	65.9	58.0	41.6
PCL60ST37C3T7	58.2	65.1	58.8	42.1
PCL60ST37C3T10	57.7	65.2	57.2	41.0

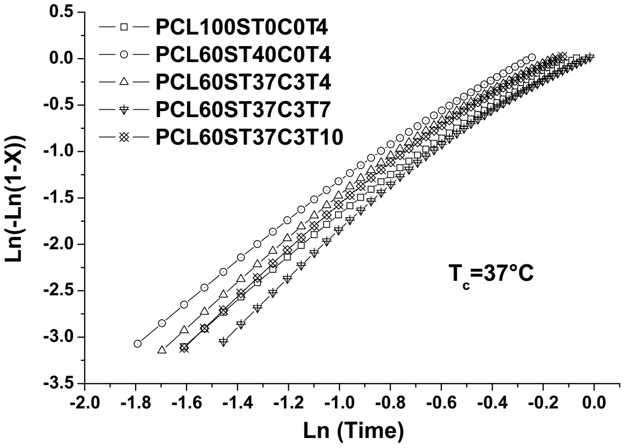

Fig. 4. Plots of log[−ln(1−X)] versus log(t) for isothermal melt crystallization at 37 °C.

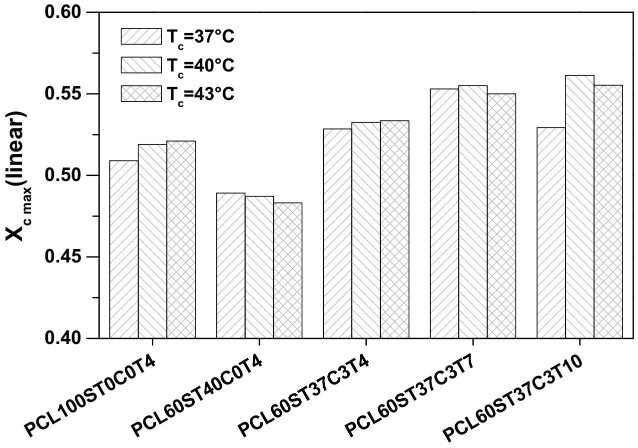

Fig. 5. Crystallinity level at which take place the deviation from the Avrami model in isothermal melt crystallization of the various samples.

overcome to reject, occlude and/or deform the dispersed non-crystallizable domains. In some cases these values produce a measurable contribution to k; for some other systems, instead, the energy barriers introduced by the presence of dispersed domains are much smaller than overall energy barrier, and the overall effect of the filler on crystallization rate is negligible.

Eq. (2) is based on a two-phase model where the radial growth rates of the crystals are assumed to be constant and the nucleation mode unique. As the crystallization proceeds and neighbouring crystallites begin to impinge, the crystallization will deviate from the Avrami expression and show a slower growth rate.

As reported in Table 3, the analysis of the isothermal data gives the Avrami exponent (n) ranging between 2.5 and 3. These results indicate that all samples crystallize with a 3-dimensional morphology, and that athermal nucleation dominates.

As shown in Fig. 4, at the crystallization temperature of 37 °C the deviation from the Avrami equation takes place at different crystallinity levels for the various blends. In immiscible polymer blends, in fact, the non-crystallizable component is segregated as a dispersed phase. This phase, during solidification, must be rejected and/or occluded by the growing spherulites, causing a supplementary contribution to the energy needed for the crystal growth.

It is quite evident from Fig. 5 that despite the crystallization temperature, the starch addition strongly reduces the crystallinity level at which the deviation happen, whereas the milling time increases this level up to crystallinity of 55%.

3.5. Mechanical properties

The tensile properties of the milled PCL and their blends with starch and clay are compared in Table 4. The effect of starch addition on mechanical properties of PCL can be clearly seen. PCL is a quite ductile polymer, able to undergo large deformations (Avella et al., 2000). In samples milled for 4 h, the addition of 40% of starch increased the Young's modulus by more than 10% in the blend, whereas the strength and elongation at break was reduced of about 50 and 80%, respectively. Similar increase in the modulus upon the addition of starch to PCL has been observed in other studies (Avella et al., 2000; Mani & Bhattacharya, 2001).

The decrease in tensile strength and elongation at break is comparable to the values reported (60%) by Avella et al. (2000) and Mani & Bhattacharya (2001). As pointed out also in these similar studies, the starch particles in the PCL matrix prevented the cold drawing that result in orientation of PLC molecules.

The addition of 3%wt. of clay produces an additional increase of the modulus. The trend is quite interesting: in fact, going from the 4 h milled to the 7 h milled sample until to 10 h one the modulus increases of about 50, 74 and 93%, respectively. Such a result indicates that the complete delamination of the clay structure is a crucial parameter for improving the mechanical properties.

In summary, the increase in the modulus can be attributed both to better interfacial adhesion between the starch and PCL and the reinforcement effect from the dispersion of the clay in the matrix. Better interfacial adhesion can be associated with the formation of a small amount of physical or chemical crosslinked species during

Table 3
Avrami model parameters for all samples analyzed

	PCL		PCL100ST0C0T4		PCL60ST40C0T4		PCL60ST40C3T4		PCL60ST40C3T7		PCL60ST40C3T10	
Tc [°C]	n	k [min^{-n}]	n	k [min^{-n}]	n	k [min^{-n}]	n	k [min^{-n}]	n	k [min^{-n}]	n	k [min^{-n}]
37	2.51	0.872	2.21	3.633	2.14	4.894	2.27	4.744	2.46	4.887	2.37	4.669
40	2.69	0.08	2.53	0.473	2.43	0.532	2.81	0.467	2.85	0.465	2.86	0.388
43	2.8	0.005	2.52	0.04	2.32	0.075	2.91	0.026	2.55	0.045	2.8	0.031
45	2.52	0.002	2.26	0.012	2.38	0.012	3.11	0.003	3	0.002	2.46	0.007

Table 4
Mechanical properties of the analyzed samples

Sample	PCL100ST0C0T4	PCL60ST40C0T4	PCL60ST40C3T4	PCL60ST40C3T7	PCL60ST40C3T10
Young's modulus [MPa]	282.33	320.00	420.00	490.00	543.33
Strain at the yield [%]	0.17	0.04	0.04	0.01	0.01
Stress at the yield [MPa]	12.35	6.56	7.06	5.37	5.45
Resilience [10^{-3} J/mm^{-3}]	1.68	0.16	0.16	0.05	0.04
Strain at the break [%]	6.66	1.35	1.36	0.81	0.73
Toughess [10^{-3} J/mm^{-3}]	69.99	5.92	5.02	2.08	1.39

the milling process. This could include starch–starch, PCL–PCL and starch–PCL crosslinks.

3.6. Dynamic mechanical properties

Figs. 6 and 7 show the tensile storage (E') and tensile loss modulus (E''), resulting from the DMA characterization of the various samples. Only the most characteristic and interesting curves are presented.

Starch addition as well as the milling time increases the storage modulus in the blends in the entire temperature region. The glass transition temperature (identified as the temperature where the loss modulus and the tan δ present a peak) increases on increasing the milling time.

However, the increase in the glass transition of the blends is difficult to explain. It probably corresponds to an overlapping of different effects related to the glass transition of PCL matrix, secondary relaxation of starch, crosslinking between starch and PCL molecules and polymer clay interactions. Moreover the increased intercalation of PCL and starch into the clay sheets with an increasing milling time could produce a decrease in the chains mobility. The increase in the peak widths of the composites could explain to some extent also the worse elongational properties.

3.7. Transport properties

The transport properties of a liquid or a vapor in a polymer are defined as the sorption and the diffusion of a solvent molecule across the amorphous phase. In filled polymers, described as two-phase systems, the inorganic filler particles are considered to be impermeable to the vapor molecules, which are thus compelled to diffuse and absorb only in the polymer regions. Therefore by increasing the crystallinity, there is a decrease in sorption due to a reduced amorphous volume and a decrease in diffusion due to a more tortuous path for the diffusing molecules that must bypass impermeable crystallites (Peterlin, 1975; Roger, 1985, chap. 2).

Morphology and microstructure of this multi-phase system are expected to play a very important role in determining the transport phenomena. For instance, the presence of the inorganic layers can introduce specific sites in which permeant molecules can be entrapped. These sites increase to a large extent the sorption of the system. Indeed for composites of polycaprolactone with inorganics, as well as in the case of many other polymers, it was always found that the improvement of barrier properties was largely dominated by a decrease of the diffusion parameter (Sorrentino, Tortora, & Vittoria, 2006; Sorrentino, Gorrasi, Tortora, & Vittoria, 2006, chap. 11).

In our case, the transport properties were measured with water vapor in a range of activities from 0.2 to 0.6. Measuring the increase of weight with time for the samples exposed to the vapor at a given partial pressure, p, we obtain both the equilibrium value of the sorbed vapor, C_{eq} and the diffusion coefficient D. In fact, plotting C_t/C_{eq} as a function of square root of time and assuming Fickian behavior, the mean diffusion coefficient is derived from the linear part of the curve (Eq. (4)):

$$\frac{C_t}{C_{eq}} = 4 \cdot d \cdot \left(\frac{D \cdot t}{\pi}\right)^{\frac{1}{2}} \tag{4}$$

where d (cm) is the thickness of the sample, C_t is the water concentration at time t and C_{eq} is the water concentration at the equilibrium value.

In the case of Fickian behavior, the reduced sorption curve presents an initial linear behavior followed by a plateau indicating the equilibrium sorption; from the first linear part the mean diffusion coefficient, D (cm^2/s), for each vapor activity, is obtained.

For polymer-solvent systems, the diffusion parameter is usually not constant, but depends on the vapor activity, according to the empirical Eq. (5):

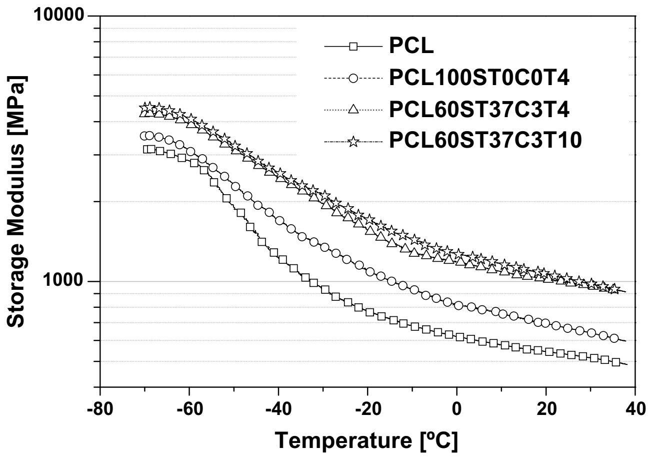

Fig. 6. Storage Modulus as a function of temperature for the reported samples.

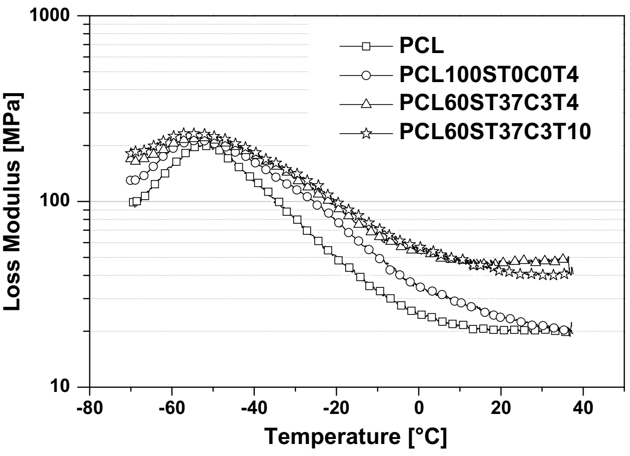

Fig. 7. Loss Modulus as a function of temperature for the reported samples.

$$D = D_0 \cdot \exp(\gamma \cdot C_{eq}) \tag{5}$$

where D_0 (cm^2/s) is the zero concentration diffusion coefficient (related to the fractional free volume and to the microstructure of the polymer); γ is a coefficient, which depends on the fractional free volume and on the effectiveness of the penetrant to plasticize the matrix. Both these parameters are related to the fractional free volume and hence to the mobility of the sorbing phase (Koenig & Huang, 1995), therefore they are useful, as widely demonstrated (Peterlin, 1975; Roger, 1985, chap. 2), in providing information on the thermo-dynamic state of permeable phase. As already observed (Gorrasi et al., 2003) the exfoliation of the inorganic component in the continuous polymeric phase is a pre-requisite to improve the barrier properties of the material to the water vapor. In the micro-composites or in the intercalated samples the ordered structure of the inorganic component does not constitute an efficient barrier to the diffusion of the water molecules that can jump from one specific site to another. In contrast, this diffusion mechanism is not possible when the structure is exfoliated, since there is no continuity in the inorganic phase.

In this case, all the analyzed samples show a linear dependence of diffusion on concentration, so it was possible to obtain the thermodynamic diffusion coefficient, D_0, by extrapolating to zero vapor concentration, in according with Eq. (5). The numerical values for all the samples are reported in Fig. 8, where the log D_0 as function of the milling time is reported. In the same figure the log D_0 of PCL and of PCL–starch blend milled for 4 h are reported as horizontal straight lines. The three composites show a thermo-dynamic diffusion coefficient much lower than the pure PCL. Moreover the decreasing of such parameter is correlated to the exfoliation of the clay: the more extended is the clay delamination the lower is the diffusion value, as observed in the case of the mechanical properties, too.

4. Conclusions

The influence of milling conditions on the structure and physical properties of PCL–starch–clay composites has been investigated by different method, giving the following results:

- The chosen milling conditions does not influence the PCL crystalline structure, neither when it is pure nor in blends with starch and clay.
- In the composite blends, the peak at $2\theta = 6.80°$, relative to the inorganic phase, appears reduced in intensity going from 4 h to 7 h of milling, and disappears for the composite milled for 10 h. An evident and gradual change of the clay organization following the milling time is observed.

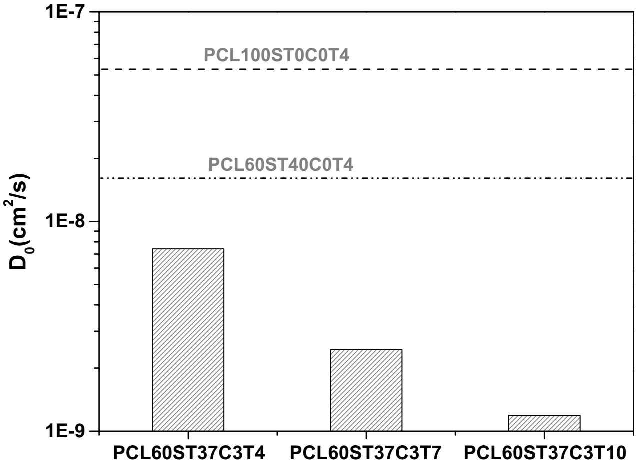

Fig. 8. Thermo-dynamic diffusion coefficients of water vapour for the various samples.

- Scanning electron microscopy shows that the milling process of PCL–starch–clay mixture for 10 h improves the interconnection between the PCL and the starch phases.
- The thermal degradation of PCL–starch blend is not influenced by the milling process. The addition of 3% of clay seems to influence only the step associated with the PCL degradation.
- The addition of 3%wt. of clay produces an increase of the elastic modulus of the PCL-starch blend. Moreover going from the micro-composite to the partially exfoliated sample up to the exfoliated one the modulus increases of about 50, 74 and 93%, respectively. Such a result indicates that the complete delamination of the clay structure is a crucial parameter for improving the mechanical properties.
- Dynamic mechanical tests show that the increased intercalation of PCL and starch into the clay sheets produce a decrease in the chains mobility.
- The thermo-dynamic diffusion coefficient for the water transport in the composites is much lower than in the pure PCL. Also the decrease of such parameter is correlated to the dispersion of the clay: indeed the more extended is the delamination the lower is the diffusion value.

In conclusion, the milling process is a promising compatibilization method for PCL–starch systems and at the same time it is a useful tool to improve the dispersion of nanoparticles into the polymer blends. A better dispersion of the clay particles, as well as a good compatibilization between PCL and starch can improve both mechanical and barrier properties.

References

Alexandre, M., & Dubois, P. (2000). Polymer layered silicate nanocomposites preparation, properties and uses on a new class of materials. *Materials Science and Engineering R – Report, 28*, 1–11.

Avella, M., Errico, M. E., Laurienzo, P., Martuscelli, E., Raimo, M., & Rimedio, R. (2000). Preparation and characterisation of compatibilised polycaprolactone/starch composites. *Polymer, 41*(10), 3875–3881.

Cavalieri, F., Padella, F., & Bourbonneux, S. (2002). High-energy mechanical alloying of thermoplastic polymers in carbon dioxide. *Polymer, 43*, 1155–1161.

Crescenzi, V., Manzini, G., Calzolari, G., & Borri, C. (1972). Thermodynamics of fusion of poly-β-propiolactone and poly-ε-caprolactone. Comparative analysis of the melting of aliphatic polylactone and polyester chains. *European Polymer Journal, 8*, 449–463.

De Kesel, C., Vander Wauven, C., & David, C. (1997). Biodegradation of polycaprolactone and its blends with poly(vinylalcohol) by micro-organisms from a compost of house-hold refuse. *Polymer Degradation and Stability, 55*, 107–113.

Felder, R. M., & Huvard, G. S. (1980). Permeation, diffusion, and sorption of gases and vapors. *Methods of Experimental Physics, 16*(Polymers, Pt. C), 315–377.

Flemming, H. C. (1998). Relevance of biofilms for the biodeterioration of surfaces of polymeric materials. *Polymer Degradation and Stability, 59*, 309–315.

Giannelis, E. P. (1996). Polymer layered silicate nanocomposites. *Advanced Materials, 8*(1), 29–35.

Gorrasi, G., Sarno, M., Di Bartolomeo, A., Sannino, D., Ciambelli, P., & Vittoria, V. (2007). Incorporation of carbon nanotubes into polyethylene by high energy ball milling: Morphology and physical properties. *Journal of Polymer Science Part B-Polymer Physics, 45*(5), 597–606.

Gorrasi, G., Tortora, M., Vittoria, V., Pollet, E., Lepoittevin, B., Alexandre, M., et al. (2003). Vapor barrier properties of polycaprolactone layered silicate nanocomposites: Effect of clay dispersion. *Polymer, 44*, 2271.

Hung, S. J., & Edelman, P. G. (1995). An overview of biodegradable polymers and biodegradation of polymers. In G. Scott & D. Gilead (Eds.), *Degradable polymers: Principles and application* (pp. 8–24). London: Chapman & Hall.

Koenig, M. F., & Huang, S. J. (1995). Biodegradable blends and composites of polycaprolactone and starch derivatives. *Polymer, 36*, 1877–1882.

Lepoittevin, B., Devalckenaere, M., Pantoustier, N., Alexandre Kubies, D., Calberg, C., Jerome, R., et al. (2002). Poly(ε-caprolactone)/clay nanocomposites prepared by melt intercalation: Mechanical, thermal and rheological properties. *Polymer, 43*, 4017–4023.

Li, S., & Vert, M. (1995). Biodegradation of aliphatic polyester. In G. Scott & D. Gilead (Eds.), *Degradable polymers: Principles and application* (pp. 3–76). London: Chapman & Hall.

Mangiacapra, P., Gorrasi, G., Sorrentino, A., & Vittoria, V. (2006). Biodegradable nanocomposites obtained by ball milling of pectin and montmorillonites. *Carbohydrate Polymers, 64*, 516–523.

Mani, R., & Bhattacharya, M. (2001). Properties of injection moulded blends of starch and modified biodegradable polyesters. *European Polymer Journal, 37*, 515–526.

Nakayama, A., Kawasaki, N., Maeda, Y., Arvanitoyannis, I., Ariba, S., & Yamamoto, N. (1997). Study of biodegradability of poly(δ-valerolactone-co-L-lactide)s. *Journal of Applied Polymer Science, 66*, 741–748.

Nesarikar, A. R., Khait, K., & Mirabella, F. (1997). Self-compatibilization of polymer blends via novel solid-state shear extrusion pulverization. *Journal of Applied Polymer Science, 63*, 1179–1187.

Orhan, Y., & Büyükgüngör, H. (2000). Enhancement of biodegradability of disposable polyethylene in controlled biological soil. *International Biodeterioration & Biodegradation, 45*, 49–55.

Oya, A., Kurokawa, Y., & Yasuda, H. (2000). Factors controlling mechanical properties of clay mineral/polypropylene nanocomposites. *Journal of Materials Science, 35*, 1045–1050.

Pan, J., & Shaw, W. J. D. (1994). Properties of a mechanically processed polymeric material. *Journal of Applied Polymer Science, 52*, 507–514.

Peterlin, A. (1975). Dependence of diffusive transport on morphology of crystalline polymers. *Journal of Macromolecular Science-Physics, B11*(1), 57–87.

Rogers, C. E. (1985). Permeability of gases and vapours in polymers. In J. Comyn (Ed.), *Polymer permeability* (pp. 11–71). UK: Elsevier.

Smith, A. P., Shay, J. S., Spontak, R. J., Balik, C. M., Ade, H., Smith, S. D., et al. (2000). High-energy mechanical milling of poly(methyl methacrylate), polyisoprene and poly(ethylene-alt-propylene). *Polymer, 41*, 627I–6283.

Sondi, I., Stubicar, M., & Pravdic, V. (1997). A. Surface properties of ripidolite and beidellite clays modified by high-energy ball milling. *Colloids and Surfaces A: Physicochemical and Engineering Aspects, 127*, 141–149.

Sorrentino, A., Gorrasi, G., Tortora, M., & Vittoria, V. (2006). Barrier properties of polymer/clay nanocomposites. In Yiu-Wing Mai & Zhong-Zhen Yu (Eds.), *Polymer nanocomposites* (pp. 273–292). Cambridge: Woodhead Publishing Ltd (ISBN 81 – 3080 – 129 - 9).

Sorrentino, A., Gorrasi, G., Tortora, M., Vittoria, V., Costantino, U., Marmottini, F., et al. (2005). Incorporation of Mg–Al hydrotalcite into a biodegradable poly(ε-caprolactone) by high energy ball milling. *Polymer, 46*(5), 1601–1608.

Sorrentino, A., Tortora, M., & Vittoria, V. (2006). Diffusion behavior in polymer-clay nanocomposites. *Journal of Polymer Science Part B-Polymer Physics, 44*, 265–274.